

# Infill Criterion for Multimodal Model-Based Optimisation

Dirk Surmann  
Uwe Ligges  
Claus Weihs

October 5, 2018

Physical systems are modelled and investigated within simulation software in an increasing range of applications. In reality an investigation of the system is often performed by empirical test scenarios which are related to typical situations. Our aim is to derive a method which generates diverse test scenarios each representing a challenging situation for the corresponding physical system.

From a mathematical point of view challenging test scenarios correspond to local optima. Hence, we focus to identify all local optima within mathematical functions. Due to the fact that simulation runs are usually expensive we use the model-based optimisation approach with its well-known representative efficient global optimisation. We derive an infill criterion which focuses on the identification of local optima. The criterion is checked via fifteen different artificial functions in a computer experiment. Our new infill criterion performs better in identifying local optima compared to the expected improvement infill criterion and Latin Hypercube Samples.

## 1 Introduction

Simulation software is widely used in a variety of applications. We mention two representative applications. Power transmission systems are simulated to shed light on problematic situations and how to deal with them in practice (SURMANN; LIGGES and WEIHS 2014; SURMANN; LIGGES and WEIHS 2017). Machine engineers check the behaviour of a new aircraft wing within simulation software before building it in reality. In most of such complex simulations the application is tested by applying empirical test scenarios. One possible scenario in a power network is a line fault in combination with an increased power consumption. Does the transmission system handle this situation? The aircraft wing is bent by a specific angle and checked for cracks after the test. After passing different test scenarios successfully the

application is deemed to be safe regarding all possible influences. However, all of these test scenarios have different points in common. Firstly, they are designed in a manual fashion. Secondly, every test scenario should reflect a challenging situation. Thirdly, the amount of test scenarios for an application should cover almost all possible situations. Finally, a simulation run is expensive in the majority of cases.

Our goal is a quality improvement of test scenarios to generate diverse test data each representing a challenged situation for an application. Due to the fact, that a simulation is expensive in its execution, we use the efficient global optimisation (EGO) approach proposed by JONES; SCHONLAU and WELCH (1998). EGO is based on a measured response from a black box function with the objective to find its global optimum. An exemplary response in a transmission system could be the simulated time until the simulation of a power network fails. In the aircraft wing example we can use the number of cracks or their averaged length. Multi-objective model-based optimisation (BISCHL; WESSING, et al. 2014) covers multiple responses.

EGO and model-based optimisation (MBO) mainly focus on global optimisation. BISCHL; RICHTER, et al. (2017) give an overview of state of the art techniques regarding multi-objective MBO using parallel computing. An additional criterion for multi-objective optimisation is given by BISCHL; WESSING, et al. (2014). The topic at hand obtains a set of good solutions in contrast to a single global optimum. WESSING and PREUSS (2017) discussed the search for multiple optima instead of a global one. By using all samples from EGO rating them via topographical selection (TÖRN and VIITANEN 1992) the approach is capable to identify different optima. In a computer experiment with twelve artificial test problems WESSING and PREUSS (2017) work out the differences between four algorithms.

The paper at hand aims to improve the efficient search of multiple optima in expensive functions. For the sake of simplicity the focus is on local minima which can be switched to local maxima by inverting the corresponding function. [Section 2](#) describes the used methods, especially [section 2.2](#) provides a new infill criterion which aims to identify local minima. We focus to find all minima of the corresponding function. In the identification process minima with lower function values are more interesting than those with higher values. The criterion is checked in [section 3](#) via fifteen different test functions in a computer experiment. To rate the results, we work out all local minima of the artificial test functions and list them in [appendix A](#). [Section 4](#) summarises the paper in a conclusion.

## 2 Methods

This section describes the general MBO algorithm and one of its representatives, EGO, in [section 2.1](#). We introduce an infill criterion to identify local minima in [section 2.2](#). The identification of local minima within the corresponding surrogate function is described in [section 2.3](#). Rating the solutions of the different algorithms is specified in [section 2.4](#).

## 2.1 Model-Based Optimisation

Let  $f : \mathcal{X} \rightarrow \mathbb{R}$  be an arbitrary deterministic objective function with a  $p$ -dimensional numeric input domain  $\mathcal{X} = [\mathbf{l}, \mathbf{u}] \subset \mathbb{R}^p$ . The vectors  $\mathbf{l} = (l_1, \dots, l_d)^\top$  and  $\mathbf{u} = (u_1, \dots, u_d)^\top$  are the lower and upper bounds of  $\mathcal{X}$ , respectively.

The neighbourhood of a point  $\mathbf{x}^* \in \mathcal{X}$  is defined by  $N(\mathbf{x}^*) = \{\mathbf{x} \in \mathcal{X} | d(\mathbf{x}, \mathbf{x}^*) \leq \epsilon\}$  with  $\epsilon > 0$  and a metric  $d : \mathcal{X} \times \mathcal{X} \rightarrow \mathbb{R}^+$ .  $f(\mathbf{x}^*)$  is a local minimum if  $\exists \epsilon > 0 : \nexists \mathbf{x} \in N(\mathbf{x}^*) : f(\mathbf{x}) < f(\mathbf{x}^*)$ . As described by WESSING and PREUSS (2017) this definition ensures the global minimum to be a local minimum, even if it includes all plateaus. All local minima are summarised in the solution set  $S = \{\mathbf{x} \in \mathcal{X} | f(\mathbf{x}) = f(\mathbf{x}_i^*)\}$  where  $f(\mathbf{x}_i^*)$  are the  $i = 1, \dots, h$  local minima of the objective of the test function. For the sake of simplicity, we are interested in all local minima of the given test function. A definition to restrict the number of minima to a given value can be found in WESSING and PREUSS (2017, sec. 2) as well as some brief ideas on additional constraints for the solution set.

Model-based optimisation (MBO) is usually used in an environment where  $f$  is expensive to evaluate, hence only a limited number of function evaluations is allowed. In every iteration  $f$  is approximated via a much cheaper to evaluate surrogate model (or meta-model)  $\hat{f}$ . The general MBO approach is outlined in the following list and is described in depth by BISCHL; RICHTER, et al. (2017).

1. Generate an initial design  $D \subset \mathcal{X}$  (usually Latin Hypercube Design (MCKAY; BECKMAN and CONOVER 1979)) and calculate  $\mathbf{y} = f(D)$ .
2. The sequential phase starts fitting a surrogate model to the evaluated points  $D$  and the corresponding values  $\mathbf{y}$ .
3. Get additional point  $\mathbf{x}'$  proposed by infill criterion (see section 2.2). The criterion works on  $\hat{f}$  and determine points which are promising for optimisation.
4. Evaluate  $\mathbf{x}'$  to  $\mathbf{y}'$  using  $f$  and extend  $D$  and  $\mathbf{y}$ , respectively.
5. If no termination criteria are met (number of evaluations, etc.) go to step 2.
6. Return  $\hat{\mathbf{y}}^* = \min(\mathbf{y})$  and corresponding  $\hat{\mathbf{x}}^*$  as proposed global optimum for  $f$ .

Step 2 of the MBO approach fits a surrogate model as a cheaper to evaluate function to the current design  $D$  with respect to the evaluations  $\mathbf{y}$ . The model choice has a main effect on the approximation of the objective function. Because  $\mathcal{X} \subset \mathbb{R}^d$  KRIGING (JONES; SCHONLAU and WELCH 1998; WILLIAMS and RASMUSSEN 2006) is recommended and provides a direct estimation of the prediction standard error, or local uncertainty measure, next to the estimation of the true function value  $f(\mathbf{x})$ . For instance, EGO is a well known KRIGING based approach.

## 2.2 Gradient Enhanced Inspection of Local Minima

The infill criterion is another essential part of MBO. It leads the optimisation to handle the trade-off between exploitation and exploration by using a combination of different statistics from the surrogate model  $\hat{f}$ . In most situations the estimators  $\hat{\mu}(\mathbf{x})$  and  $\hat{\sigma}(\mathbf{x})$ , estimated by  $\hat{f}$  are used in a single formula to handle the trade-off in a well-balanced manner. JONES; SCHONLAU and WELCH (1998) proposed the expected improvement  $EI(\mathbf{x})$  as infill criterion, which is the most popular criterion and widely used. It is defined as  $EI(\mathbf{x}) := E(\max\{\hat{\mathbf{y}}^* - Y(\mathbf{x}), 0\})$ ,

where  $Y(\mathbf{x})$  is a random variable that expresses the posterior distribution at  $\mathbf{x}$ , estimated via the surrogate model  $\hat{f}$ . Using a KRIGING model  $Y(\mathbf{x})$  is normally distributed with  $Y(\mathbf{x}) \sim \mathcal{N}(\hat{\mu}(\mathbf{x}), \hat{s}^2(\mathbf{x}))$ . Using this assumption,  $EI(\mathbf{x})$  can be expressed as

$$EI(\mathbf{x}) = (\hat{y}^* - \hat{\mu}(\mathbf{x})) \Phi\left(\frac{\hat{y}^* - \hat{\mu}(\mathbf{x})}{\hat{s}(\mathbf{x})}\right) + \hat{s}(\mathbf{x}) \phi\left(\frac{\hat{y}^* - \hat{\mu}(\mathbf{x})}{\hat{s}(\mathbf{x})}\right) \quad (1)$$

where  $\phi$  and  $\Phi$  are the density and distribution function of the standard normal distribution, respectively. In the first addend the difference between the current minimum  $\hat{y}^*$  and the local estimator  $\hat{\mu}(\mathbf{x})$  is rated high for lower values of  $\hat{\mu}(\mathbf{x})$ . Its corresponding standard deviation  $\hat{s}(\mathbf{x})$  is rated high for its higher values. Hence, the expected improvement leads us to points with low  $\hat{\mu}(\mathbf{x})$  and high  $\hat{s}(\mathbf{x})$ .

Simpler approaches to compound  $\hat{\mu}(\mathbf{x})$  and  $\hat{s}(\mathbf{x})$  for a point  $\mathbf{x}$  are given by the lower confidence bound ( $LCB(\mathbf{x})$ ) or the standard error ( $SE(\mathbf{x})$ ) itself in [equation \(2\)](#), where  $\lambda > 0$  is a constant to control the trade-off between both estimators in [equation \(2a\)](#).

$$LCB(\mathbf{x}; \lambda) = \hat{\mu}(\mathbf{x}) - \lambda \hat{s}(\mathbf{x}) \quad (2a)$$

$$SE(\mathbf{x}) = \hat{s}(\mathbf{x}) \quad (2b)$$

The infill criterion  $SE(\mathbf{x})$  in [equation \(2b\)](#) handles the trade-off by shifting the whole weight to exploration. It will try to cover the design space of the objective function equally, to reduce the local standard error.

Our purpose to inspect local minima yields a modified form of  $EI(\mathbf{x})$  and  $SE(\mathbf{x})$ . We search for meaningful test scenarios to challenge the corresponding application. This usually results in lower values of the response function compared to non-challenging test scenarios. A meaningful test scenario is translated into the model-based optimisation as a local minimum whose function value is near to the global minimum. The slope at a point between two local minima has to be significantly different from 0, otherwise it is a plateau which is considered as one minimum. Hence, we enhance the new infill criterion to skip exploration in regions with a steep surrogate function. The gradient enhanced inspection of local minima  $GEILM(\mathbf{x})$ , as new infill criterion, is defined by

$$GEILM(\mathbf{x}) = \hat{s}(\mathbf{x}) \Phi\left(\frac{\hat{y}^* - \hat{\mu}(\mathbf{x})}{s_p}\right) g_\lambda(\|\nabla \hat{\mu}(\mathbf{x})\|_\infty) \quad (3)$$

with

$$s_p = \min \left\{ s \in \mathbb{R}^+ \mid \frac{\hat{y}^* - \max(\mathbf{y})}{s} = \Phi^{-1}(p) \right\} \quad (4)$$

where  $\Phi$  is the distribution function of the standard normal distribution.  $g_\lambda$  is the density of the exponential distribution with parameter  $\lambda$ .  $\|\cdot\|_\infty$  describes the supremum norm of  $\cdot$  and is called maximum norm in case of a vector  $\mathbf{a} = (a_1, \dots, a_n)^\top$ . In this case it takes the form  $\|\mathbf{a}\|_\infty = \max\{|a_1|, \dots, |a_n|\}$ . The differential operator, or nabla operator,  $\nabla$  is defined in terms of partial derivative operators and denotes the gradient of a scalar field. We choose  $SE(\mathbf{x})$

with its explorative nature as a starting point and use the multiplication operator to implement a weighting on  $SE(\mathbf{x})$ . Summing up the coefficients is only meaningful for infill criteria which deal with  $\hat{\mu}(\mathbf{x})$  directly and do not cover  $\hat{\mu}(\mathbf{x})$  in a function, as shown in [equations \(1\) and \(2a\)](#), because  $\hat{\mu}(\mathbf{x})$  is related to exploitation whereas  $\hat{s}(\mathbf{x})$  is related to exploration. The weighting via  $\Phi$  is reused from  $EI(\mathbf{x})$  to add a connection to the expected function value  $\hat{\mu}(\mathbf{x})$ .  $\Phi$  weights down  $\hat{\mu}(\mathbf{x})$  the more it differs from the current minimum  $\hat{y}^*$  which reflects the higher interest in local minima with lower function values. We adjust the standardisation via a  $p$ -quantile standard deviation  $s_p$  with  $p \in (0, 1)$ .  $s_p$  is driven by the range of evaluated design points and independent of  $\hat{s}(\mathbf{x})$ . This approach supports  $GEILM(\mathbf{x})$  exploring the design space with higher expected values  $\hat{\mu}(\mathbf{x})$  with a lower priority. Due to the fact that a gradient at a point between two optima is significantly different from 0 we add a second weighting via the exponential distribution  $g_\lambda$ . It considers the maximum partial derivative to ensure the highest weighting for local optima. Design points outside local optima (or plateaus) get lower priority which further enhances  $GEILM(\mathbf{x})$  to use the available number of runs in promising regions.

Two exemplary design points illustrate the behaviour of  $GEILM$ . In the global minimum  $\hat{y}^*$  the total weight on  $\hat{s}(\mathbf{x})$  evaluates to its maximum of  $\frac{1}{2}\lambda$ . In this case  $\Phi$  evaluates to  $\frac{1}{2}$  and  $g_\lambda$  to  $\lambda$  because the gradient in an optimum is 0. Hence,  $GEILM(\mathbf{x})$  evaluates to  $\frac{1}{2}\lambda\hat{s}(\mathbf{x})$  for the global minimum. If we assume an example point which is not a local minimum, with a high value of the local estimator compared to the global minimum,  $GEILM(\mathbf{x})$  converges to 0. The function  $\Phi$  converges to 0 for higher values of  $\hat{\mu}(\mathbf{x})$ . The function  $g_\lambda$  converges to 0 for increasing absolute values of the gradient. If the surrogate function is unexplored at this point  $\hat{s}(\mathbf{x})$  updates the infill criterion  $GEILM(\mathbf{x})$ .

### 2.3 Identify Local Minima of Surrogate Function

Identifying the local minima after performing the model-based optimisation is done via topographical selection (TÖRN and VIITANEN 1992) by WESSING and PREUSS (2017). We follow a different approach and instead use the surrogate function of evaluated points from the objective function to identify the local minima. This method has the advantage to detect minima in areas with lower exploitation. However, the surrogate function can estimate the objective function inaccurately. To identify the local minima, we draw a Latin Hypercube Sample (STEIN 1987)  $U^* \subset \mathcal{X}$  of size  $n = 200^{\log_3(p+3-1)}$  according to the number of dimensions  $p$ . The formula for  $n$  is defined empirically to balance the expected workload and required points covering the input domain  $\mathcal{X}$  in [section 2.1](#). We apply the quasi-NEWTON algorithm with box constraints (L-BFGS-B) defined by BYRD et al. (1995) and described by NOCEDAL and WRIGHT (2006) to all points  $\mathbf{x} \in U^*$ . This gradient descent algorithm moves each point  $\mathbf{x}$  to its next local minimum  $\mathbf{x}_i^*$  of the surrogate function  $\hat{f}$  with  $i = 1, \dots, k$  local minima. We skip all points in  $U^*$  which moved to the limits of  $\mathcal{X}$  assuming the local minima of the objective function within the input domain. The approximation set  $U$  is defined by agglomerations near the representatives in  $U^*$  via

$$U = \{\mathbf{x} \in \mathcal{X} | d_{Che}(\mathbf{x}, U^*) \leq \delta\} \quad (5)$$

with  $\delta > 0$ . The function  $d_{\text{Che}}(\mathbf{x}, U^*)$  denotes the Chebyshev distance (ABELLO; PARDALOS and RESENDE 2002) of a point  $\mathbf{x}$  to its nearest neighbour in  $U^*$ .

Different approaches to identify multiple optima were applied in the field of multimodal optimisation. GUDLA and GANGULI (2005) proposed a hybrid between genetic and gradient algorithms. Evolutionary algorithms are used by DEB and SAHA (2010) in a concept of multi-objective optimisation to solve a single-objective problem. STOEAN et al. (2010) combine their genetic algorithm with a topological separation of subpopulations and apply the approach to different test functions. A hybrid of NELDER-MEAD algorithm and gradient descent method is applied by ABBAS et al. (2018) to signal processing. Our approach spreading points in the input domain via a Latin Hypercube Sample and move them to their nearest local minima is simple and empowers us to calculate large samples. Further research will show if more complex algorithms identify local optima considerably faster.

## 2.4 Rate Solution Set

Global optimisation uses the deviation from the global optimum as a performance measure. In multimodal optimisation we use the number of found local minima  $l = |U|$  divided by the correct number of optima  $|S| = h$  as peak ratio  $\text{PR}(U) = \frac{l}{h}$ . Because the surrogate function is used to identify the local minima we define the peak ratio different than URSEM (1999). They choose the set of local minima  $S$  as a reference set to check if each minimum is met by a point in the final design  $D$ . We deal with  $\mathcal{X}$  to identify the agglomerated number of found optima in  $U^*$ . Hence,  $\text{PR}(U) \in (0, \infty)$  which reveals improper fits of the surrogate functions for high values of PR.

Another measure is the averaged HAUSDORFF distance (AHD) described by HAUSDORFF (1927) and ROCKAFELLAR and WETS (2004). It is defined by

$$\text{AHD}(U) = \max \left\{ \left( \frac{1}{l} \sum_{i=1}^l d_{\text{nn}}(\mathbf{x}_i, U)^r \right)^{\frac{1}{r}}, \left( \frac{1}{h} \sum_{i=1}^h d_{\text{nn}}(\mathbf{x}_i^*, S)^r \right)^{\frac{1}{r}} \right\} \quad (6)$$

using  $S$  as a reference set. The function  $d_{\text{nn}}(\mathbf{x}, X)$  denotes the Euclidean distance of a point  $\mathbf{x}$  to a its nearest neighbour in a set of points  $X$ .

## 3 Experiment

This section describes the computer experiment to analyse the proposed infill criterion with its setup in section 3.1. Section 3.2 analysis the extreme values occur in the results. A comparison between the three methods is discussed in section 3.3.

### 3.1 Setup

We evaluate the performance of the infill criterion GEILM using an extensive computer experiment. It is compared to the most popular EI infill criterion and a Latin Hypercube Sample



(STEIN 1987) using  $n_{\text{of}} = 15$  artificial objective functions as black box functions. Table 1 contains the objective functions used in this experiment. We list the name, the dimensionality,

Table 1: Objective Functions used for Testing

Function Name	Dim.	#Local Minima	Reference
Alpine Function No. 02	1	2	Table 4
Alpine Function No. 02	2	5	Table 5
Alpine Function No. 02	3	14	Table 6
BRANIN Function	2	3	Table 7
Cosine Mixture Function	1	5	Table 8
Cosine Mixture Function	2	25	Table 9
Cosine Mixture Function	3	125	Table 10
HARTMANN Function	3	3	Table 11
HARTMANN Function	6	2	Table 12
HIMMELBLAU Function	2	4	Table 13
Modified RASTRIGIN Function	4	48	Table 14
Modified RASTRIGIN Function	8	48	Table 15
SHEKEL Function 5	4	5	Table 16
SHEKEL Function 7	4	7	Table 17
SHEKEL Function 10	4	10	Table 18

the number of local minima, and a reference for each objective function. All local minima are worked out in a computationally intensive task and tabulated in appendix A, because only data of the global minimum can be found in the literature. The set of objective functions consist of the classic test set for global optimisation by DIXON and SZEGÖ (1978), which is a subset of test problems described by ALI; KHOMPATRAPORN and ZABINSKY (2005). We expand this set by the Alpine Function No. 02 (CLERC 1999), the Cosine Mixture Function (ALI; KHOMPATRAPORN and ZABINSKY 2005), the HIMMELBLAU Function (HIMMELBLAU 1972) and the modified RASTRIGIN Function (DEB and SAHA 2012).

Model-based optimisation is split into an initial and a sequential phase (section 2.1). The number of points drawn in the initial phase is equal to  $n_{\text{init}} = \{3^2, 4^2, \dots, 8^2\}^T$ . In the sequential stage  $n_{\text{seq}} = \{3^2, 4^2, \dots, 12^2\}^T$  are added using the infill criterion. All elements in both vectors are squared, to focus on results with a lower number of design points. Designs with higher numbers are less interesting, because the real world simulations are too expensive to evaluate a high amount of design points. All combinations of elements in  $n_{\text{init}}$  and  $n_{\text{seq}}$  are evaluated in the experiment. We evaluate  $|n_{\text{init}}| \cdot |n_{\text{seq}}| \cdot n_{\text{of}} = 900$  experiments for each infill criterion. To compare the infill criteria to a Latin Hypercube Sample (LHS), we fit the same KRIGING model as in MBO to a LHS with  $n_{\text{LHS}} = \{4^2, 5^2, \dots, 15^2\}^T$  design points which results in  $|n_{\text{LHS}}| \cdot n_{\text{of}} = 180$  experiments. Each experiment is repeated 30 times which results in  $(2 \cdot 900 + 180) \cdot 30 = 59400$  runs, including infill criteria EI and GEILM. We set the hyperparameters of GEILM criterion in equations (3) and (4) to  $\lambda = 2$  and  $p = 0.001$ , respectively. Both choices were made empirically to uprate low gradients ( $\lambda$ ) and rate down extreme

values ( $p$ ). Further research can be done on these hyperparameters.

In each run we record two performance measurements to rate the solution set (section 2.4). The peak ratio (PR) which considers representatives for every local minimum in equation (5) with  $\delta = 0.001$  and the averaged HAUSDORFF distance (AHD) with  $r = 1$  in equation (6). All implementation is done in R (R DEVELOPMENT CORE TEAM 2017) via package `m1rMBO` (BISCHL; RICHTER, et al. 2017). We parallelise the experiment using package `batchtools` (LANG; BISCHL and SURMANN 2017).

### 3.2 Extreme Values

The construction of PR results in the interval  $(0, \infty)$ . However, we expect two soft limits 0 and 1. No minima are found with  $PR = 0$  whereas a value of 1 indicates that all local minima are found. Due to construction, PR is capable to detect overfitted surrogate models. If the KRIGING model finds too many optima, PR exceeds 1 and indicates overfitting by higher values. Hence, we are interested in a reasonable dataset which covers the expected interval  $[0, 1]$  as well as the overfitting indication. We choose the interval  $[0, 5]$  empirically. The value  $PR = 5$  indicates a surrogate function with five times more minima than the corresponding objective function and indicates overfitting.

A first analysis of PR shows extreme values up to 11 260.5 and points out 16.3 % runs with  $PR > 5$  as shown in table 2. The table lists the count of PR values in the corresponding

**Table 2:** Number of Extreme Values in PR Intervals

Intervall	Count
A = $[0, 5]$	49 697
B = $(5, 50]$	734
C = $(50, 500]$	2698
D = $(500, 1500]$	6259
E = $(1500, \infty)$	12

intervals. We choose these remaining interval ranges for B to E in a way to plot values of PR in histograms which illustrate the extreme values. The different information shown in figure 1 will be hidden if the data is plotted in one histogram. Extreme values are independent of the

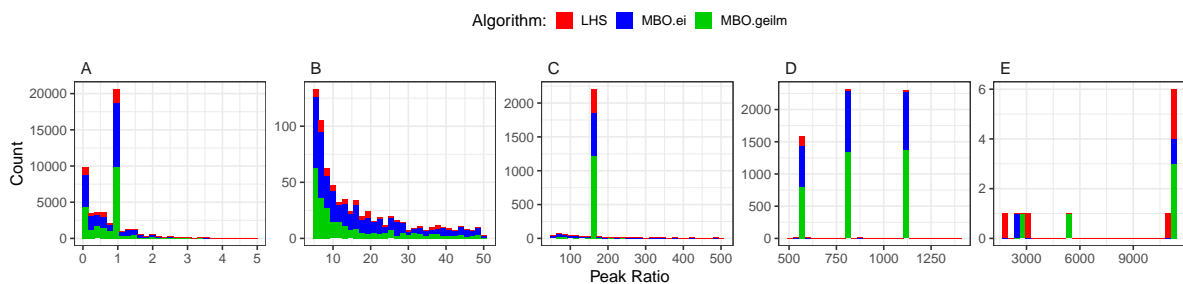


**Figure 1:** Extreme Values in PR Intervals by Algorithm



used method. Certainly, the ratio of LHS algorithm is lower, because the number of chosen MBO combinations is ten times higher. The histogram A shows two peaks indicating the soft limits 0 and 1 of PR. Higher values indicate a misleading surrogate function with too many local minima. Histogram B illustrates the exponential decrease for higher values of PR which can be observed in histogram A, too. The peaks in histograms C, D and E are far outside this decreasing histogram range described by A and B and calculated in [table 3](#). Apparently, the

**Table 3:** Number of Extreme Values in PR by Interval and Problem

Function	Interval Counts				
	B	C	D	E	B – E
Alpine02.2	3	130			133
Alpine02.3	79	2087			2166
CosineMix.3	4				4
Hartmann.3			1		1
Hartmann.6	26	12	6	12	56
Himmelblau		2			2
modRastrigin.4	2	2			4
modRastrigin.8	2	3	1		6
Shekel.5	175	135	2332		2642
Shekel.7	154	152	2339		2645
Shekel.10	289	175	1580		2044

Alpine Function No. 02 and the SHEKEL Functions 5, 7, and 10 seem to be difficult to fit, they generate nearly all extreme values. A closer look does not reveal any relation to the number of design points, neither the number of initial points nor the number of sequential points. The divergence in these functions is spread through the complete experimental space. Because interval B contains only functions discovered in C to E, we decide to refer the further analysis to interval A.

### 3.3 Comparison of Infill Criteria

[Figures 2](#) and [3](#) illustrate the progress of the two performance measurements over the number of design points. In all figures, the curves represent a local regression (LOESS) for smoothing points in scatterplots described in CLEVELAND; GROSSE and SHYU (2017) with a smoothing parameter  $\alpha = 0.5$ . The parameter  $\alpha$  controls the fraction of the neighbouring data points which are used to fit each local polynomial. Each curve is shown with a grey 95% confidence interval for the smoothed value assuming a normal distribution.

For most objective functions the proposed infill criterion GEILM beats EI in terms of peak ratio (PR), shown in [figure 2](#). It converges earlier to the optimal value of 1 which can be seen especially for Alpine Function No. 02, Cosine Mixture Function and HARTMANN Function. Especially, HARTMANN Function in 6 dimensions shows the need for an infill criterion designed to identify local minima. EI diverges over the number of design points contrary to the proposed criterion which identifies in average the correct number of local minima. This

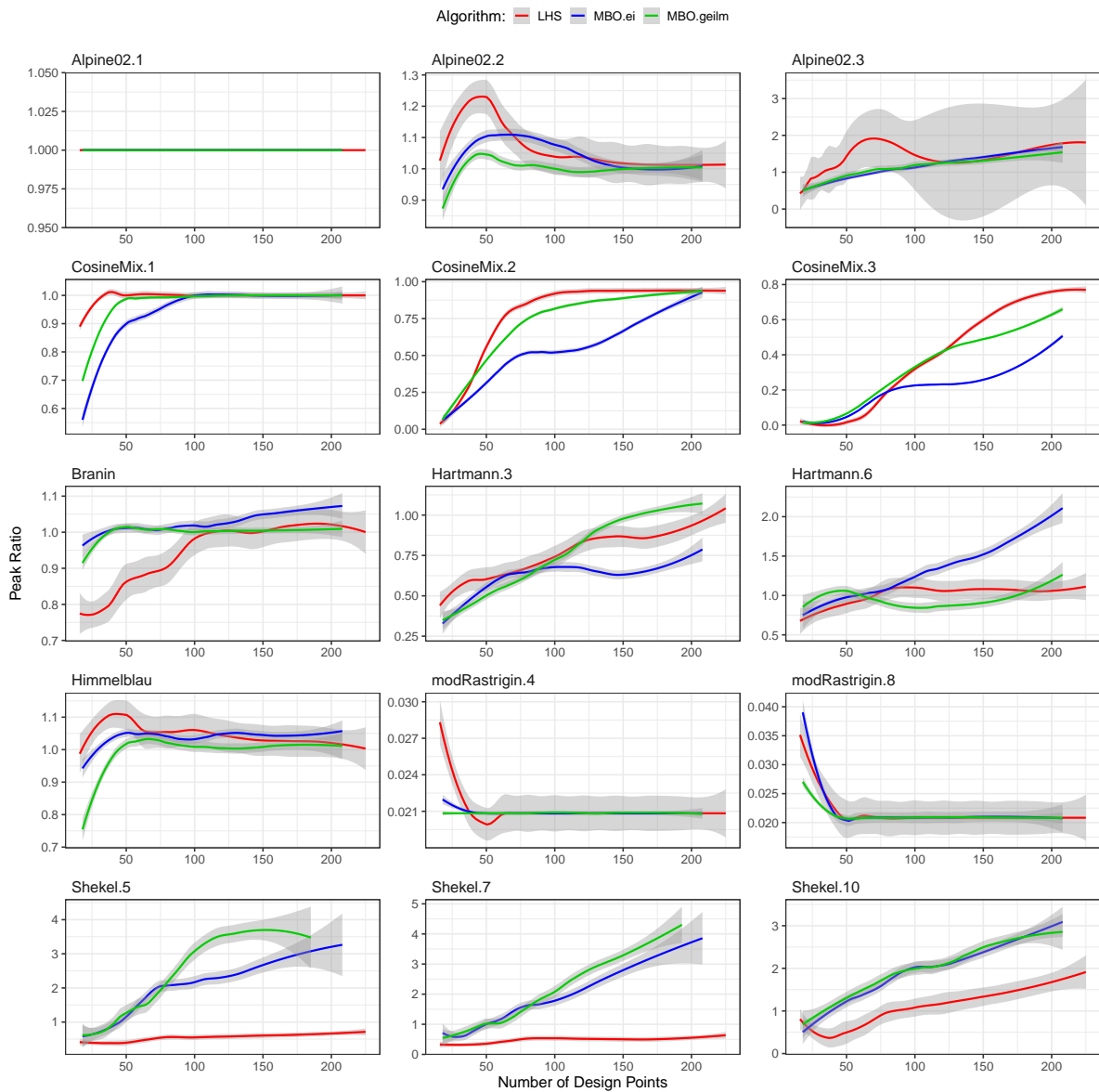


**Figure 2:** Peak Ratio (PR) over Number of Design Points Grouped by Algorithm

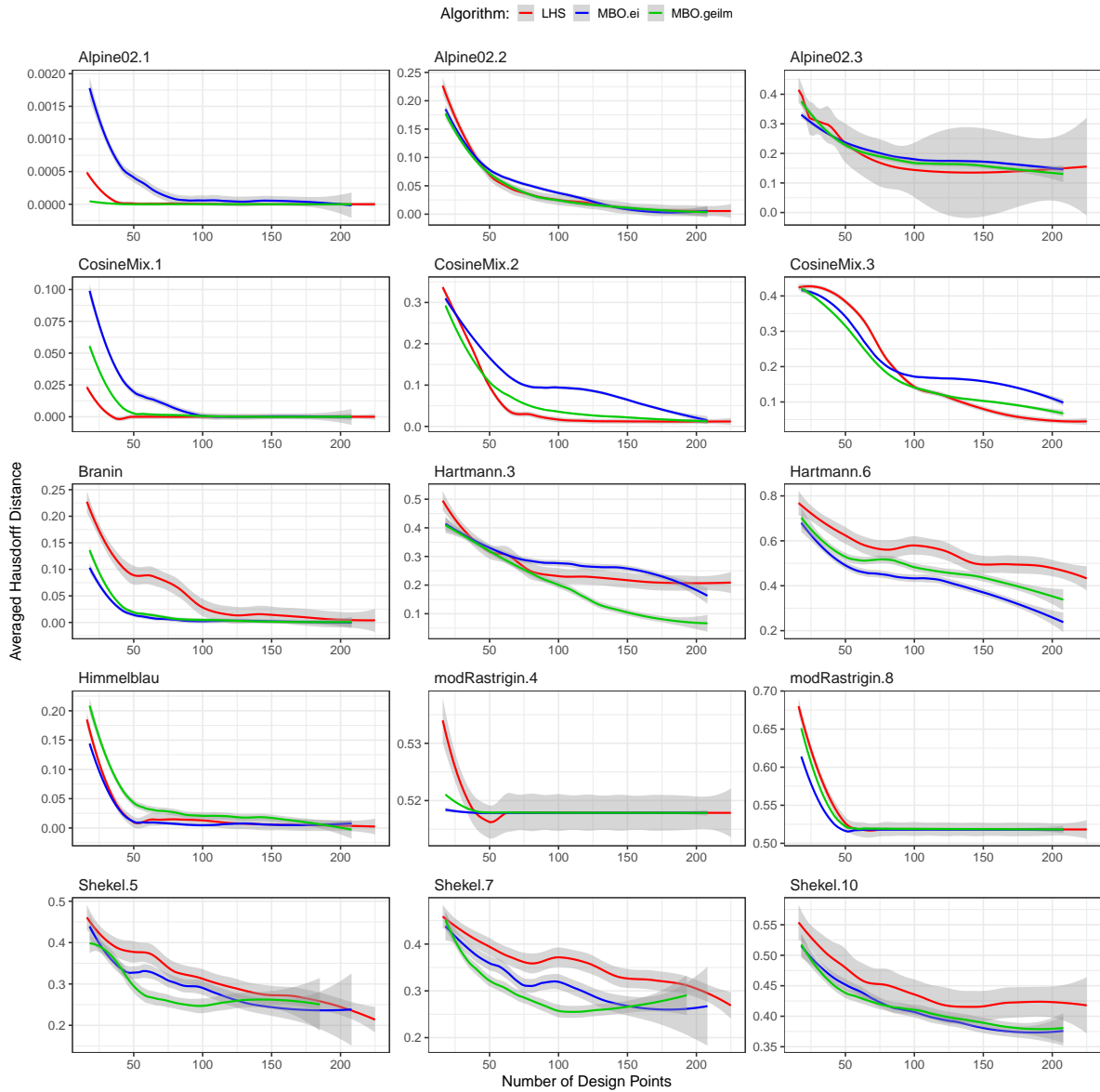


**Figure 3:** Averaged HAUSDORFF distances (AHD) over number of design points grouped by algorithm

example illustrates that EI identifies the global optimum, as expected. BRANIN, HARTMANN, and HIMMELBLAU Function illustrates the high variance of LHS. The smoothed mean of LHS outperforms MBO in many objective functions. However, the confidence intervals are often much wider compared to MBO methods. Additionally, LHS has plateaus in the BRANIN Function or overshoots in the HIMMELBLAU Function and Alpine Function No. 02 in dimensionalities 2 and 3. [Figure 3](#) shows a similar picture for the averaged HAUSDORFF distance. We reach the optimal value of  $AHD = 0$  with GEILM continuously faster than by using EI or LHS. Latin Hypercube Sampling is sometimes better in terms of mean AHD but shows a higher variance compared to the MBO approach.

All three methods are highly overstrained with the objective functions Modified RASTRIGIN and SHEKEL. The latter one was already identified in [section 3.2](#), where it generates about  $\frac{3}{4}$  of the extreme values. Whereas AHD results in lesser values with more design points, we see the divergence of PR in [figure 2](#) for all SHEKEL Functions. For the modified RASTRIGIN Function low values of PR illustrate the overstrained behaviour to identify the local minima. Only 1 of 48 local minima is identified for this type of objective functions. We suppose a problematic fit of KRIGING models to a modified RASTRIGIN Function. From our point of view, the dimension or number of local minima is not the only cause for these results, since the Cosine Mixture Function in 3 dimensions with 125 local minima shows a good performance in PR and AHD as well as HARTMANN Function in 6 dimension with 2 local optima.

In case of MBO, we are interested in the development of performance measurements over the number of initial and sequential design points. Contour plots of peak ratio over the number of initial and sequential design points, smoothed by LOESS, are shown in [figure 4](#) for infill criterion GEILM. The contour plot of averaged HAUSDORFF distance is shown in appendix [figure 5](#). We chose Alpine Function No. 02 in 2 dimensions, Cosine Mixture Function in 3 di-

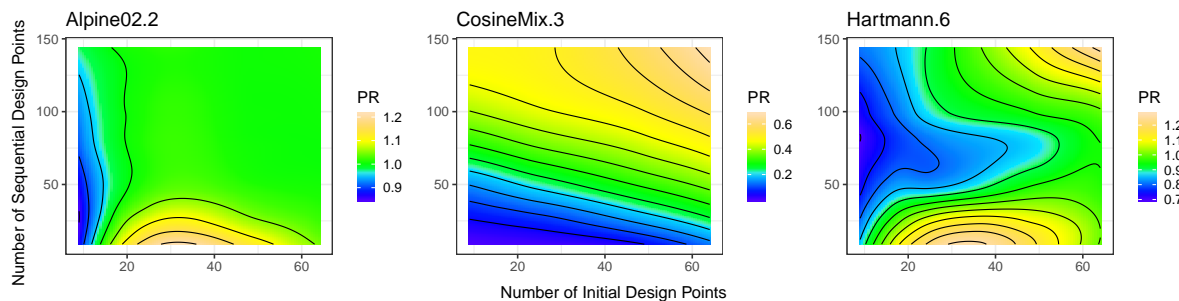


**Figure 4:** Contour Plot of Peak Ratio (PR) over Number of Initial and Sequential Design Points for Infill Criterion GEILM.

mensions and HARTMANN Function in 6 dimensions as showcases because the corresponding plots illustrate the variety of contours between the different objective functions. Contour plots of both performance measurements for all objective functions are given in appendix [figures 6](#) and [7](#). Local minima of the 2 dimensional function Alpine02 are found fast with a low number of initial and sequential points. Interestingly, a higher number of points in the initial design results in  $PR > 1$  which indicates an overfitted KRIGING model. The overfit is resolved in the sequential stage with a low number of design points. An undersized initial design is hard

to compensate because MBO needs a high number of design points in the sequential stage to achieve  $PR = 1$ . Cosine Mixture Function in 3 dimensions is an example of an expected contour plot for PR. A higher number of points in the initial or sequential design results in a constant improvement of peak ratio. A modified behaviour of Alpine02 can be found in the contour plot of HARTMANN Function in 6 dimensions. We see an overfitted surrogate model with 35 initial design points and the minimum number of points in the sequential stage. The same reaction holds for the highest amount of initial and design points which was observed in [figure 2](#) as an increase in the curve of GEILM for a high number of design points. Medium number of points in the sequential stage sometimes result in an incorrect number of local minima from the KRIGING model. This has a strong impact in LOESS because the peak ratio for a function with 2 local minima has a precision of 0.5. The corresponding contour plot of averaged HAUSDORFF distance in [figure 5](#) underlines this statement. Improvements of AHD for increasing number of points in the initial and sequential stage are illustrated by contour plots for each objective function (see [figure 7](#)).

## 4 Conclusion

We introduce the infill criterion gradient enhanced inspection of local minima (GEILM) for model-based optimisation (MBO) which aims to identify local minima in expensive objective functions. It is capable to identify all local minima and focuses on minima with lower values of the objective function. Minima with lower values are explored more intense than minima with higher function values. A computer experiment compares the behaviour of GEILM to the most popular infill criterion expected improvement (EI) used in efficient global optimisation (EGO). Additionally, we include Latin Hypercube Sampling (LHS) which reflects a state of the art design for computer experiments not considering the objective function. We work out and tabulate all local minima of the used objective functions. A variety of objective functions is tested and shows a good performance of GEILM in case of the measurements peak ratio (PR) and averaged HAUSDORFF distance (AHD). It outperforms EI and LHS in the averaged performance measurements and especially the latter in terms of variance. The need for special infill criteria to identify local minima instead of the global minimum is obvious by considering the HARTMANN Function in 6 dimensions. PR diverges using EGO over an increasing number of design points contrary to GEILM which identifies the correct number of local optima. From our point of view, it is worth the effort to define criteria purpose-built for dealing with local minima.

Future work should examine the hyperparameters of GEILM and improve the criterion to minimise the number of hyperparameters. Additionally, we may investigate the used surrogate model in MBO because of its poor behaviour with respect to the objective functions Alpine Function No. 02 and SHEKEL Functions 5, 7, and 10. Finally, the infill criteria and used surrogate model should be tested in a larger computer experiment with additional objective functions especially of higher dimensions ( $p \geq 6$ ) and a greater variety of function types. This will clarify the discussed issues and make stronger statements about the capabilities of the infill criteria aiming at local minima.

## **5 Acknowledgement**

This work has been funded by the Deutsche Forschungsgemeinschaft (DFG), Forschergruppe 1511 *Schutz- und Leitsysteme zur zuverlässigen und sicheren elektrischen Energieübertragung*.



## A Local Minima

This section lists all local minima of the used objective functions. The rows are ordered according to the function value  $y$  beginning with the global minima.

### A.1 Alpine Function No. 02

**Table 4:** Local Minima of 1-Dimensional Alpine02

#	$x$	$y$
1	7.917	-2.808
2	1.837	-1.308

**Table 5:** Local Minima of 2-Dimensional Alpine02

#	$x$	$y$	
1	7.917	7.917	-7.886
2	4.816	4.816	-4.764
3	1.837	7.917	-3.672
4	7.917	1.837	-3.672
5	1.837	1.837	-1.710

**Table 6:** Local Minima of 3-Dimensional Alpine02

#	x			y
1	7.917	7.917	7.917	-22.144
2	4.816	4.816	7.917	-13.379
3	4.816	7.917	4.816	-13.379
4	7.917	4.816	4.816	-13.379
5	1.837	7.917	7.917	-10.311
6	7.917	1.837	7.917	-10.311
7	7.917	7.917	1.837	-10.311
8	1.837	4.816	4.816	-6.230
9	4.816	1.837	4.816	-6.230
10	4.816	4.816	1.837	-6.230
11	1.837	1.837	7.917	-4.802
12	1.837	7.917	1.837	-4.802
13	7.917	1.837	1.837	-4.802
14	1.837	1.837	1.837	-2.236

## A.2 BRANIN Function

**Table 7:** Local Minima of 2-Dimensional BRANIN

#	x		y
1	-3.142	12.275	0.398
2	3.142	2.275	0.398
3	9.425	2.475	0.398

## A.3 Cosine Mixture Function

**Table 10:** Local Minima of 3-Dimensional CosineMix

#	x			y
1	0.000	0.000	0.000	-0.300
2	-0.369	0.000	0.000	-0.152
3	0.000	-0.369	0.000	-0.152
4	0.000	0.000	-0.369	-0.152
5	0.000	0.000	0.369	-0.152
6	0.000	0.369	0.000	-0.152
7	0.369	0.000	0.000	-0.152

— continue on next page —

— continued from previous page —

#	x		y	
8	-0.369	-0.369	0.000	-0.004
9	-0.369	0.000	-0.369	-0.004
10	-0.369	0.000	0.369	-0.004
11	-0.369	0.369	0.000	-0.004
12	0.000	-0.369	-0.369	-0.004
13	0.000	-0.369	0.369	-0.004
14	0.000	0.369	-0.369	-0.004
15	0.000	0.369	0.369	-0.004
16	0.369	-0.369	0.000	-0.004
17	0.369	0.000	-0.369	-0.004
18	0.369	0.000	0.369	-0.004
19	0.369	0.369	0.000	-0.004
20	-0.369	-0.369	-0.369	0.143
21	-0.369	-0.369	0.369	0.143
22	-0.369	0.369	-0.369	0.143
23	-0.369	0.369	0.369	0.143
24	0.369	-0.369	-0.369	0.143
25	0.369	-0.369	0.369	0.143
26	0.369	0.369	-0.369	0.143
27	0.369	0.369	0.369	0.143
28	-0.725	0.000	0.000	0.287
29	0.000	-0.725	0.000	0.287
30	0.000	0.000	-0.725	0.287
31	0.000	0.000	0.725	0.287
32	0.000	0.725	0.000	0.287
33	0.725	0.000	0.000	0.287
34	-0.725	-0.369	0.000	0.435
35	-0.725	0.000	-0.369	0.435
36	-0.725	0.000	0.369	0.435
37	-0.725	0.369	0.000	0.435
38	-0.369	-0.725	0.000	0.435
39	-0.369	0.000	-0.725	0.435
40	-0.369	0.000	0.725	0.435
41	-0.369	0.725	0.000	0.435
42	0.000	-0.725	-0.369	0.435
43	0.000	-0.725	0.369	0.435
44	0.000	-0.369	-0.725	0.435
45	0.000	-0.369	0.725	0.435

— continue on next page —

---

— continued from previous page —

#		x		y
46	0.000	0.369	-0.725	0.435
47	0.000	0.369	0.725	0.435
48	0.000	0.725	-0.369	0.435
49	0.000	0.725	0.369	0.435
50	0.369	-0.725	0.000	0.435
51	0.369	0.000	-0.725	0.435
52	0.369	0.000	0.725	0.435
53	0.369	0.725	0.000	0.435
54	0.725	-0.369	0.000	0.435
55	0.725	0.000	-0.369	0.435
56	0.725	0.000	0.369	0.435
57	0.725	0.369	0.000	0.435
58	-0.725	-0.369	-0.369	0.583
59	-0.725	-0.369	0.369	0.583
60	-0.725	0.369	-0.369	0.583
61	-0.725	0.369	0.369	0.583
62	-0.369	-0.725	-0.369	0.583
63	-0.369	-0.725	0.369	0.583
64	-0.369	-0.369	-0.725	0.583
65	-0.369	-0.369	0.725	0.583
66	-0.369	0.369	-0.725	0.583
67	-0.369	0.369	0.725	0.583
68	-0.369	0.725	-0.369	0.583
69	-0.369	0.725	0.369	0.583
70	0.369	-0.725	-0.369	0.583
71	0.369	-0.725	0.369	0.583
72	0.369	-0.369	-0.725	0.583
73	0.369	-0.369	0.725	0.583
74	0.369	0.369	-0.725	0.583
75	0.369	0.369	0.725	0.583
76	0.369	0.725	-0.369	0.583
77	0.369	0.725	0.369	0.583
78	0.725	-0.369	-0.369	0.583
79	0.725	-0.369	0.369	0.583
80	0.725	0.369	-0.369	0.583
81	0.725	0.369	0.369	0.583
82	-0.725	-0.725	0.000	0.875
83	-0.725	0.000	-0.725	0.875

— continue on next page —

---

---

— continued from previous page —

#		x		y
84	-0.725	0.000	0.725	0.875
85	-0.725	0.725	0.000	0.875
86	0.000	-0.725	-0.725	0.875
87	0.000	-0.725	0.725	0.875
88	0.000	0.725	-0.725	0.875
89	0.000	0.725	0.725	0.875
90	0.725	-0.725	0.000	0.875
91	0.725	0.000	-0.725	0.875
92	0.725	0.000	0.725	0.875
93	0.725	0.725	0.000	0.875
94	-0.725	-0.725	-0.369	1.022
95	-0.725	-0.725	0.369	1.022
96	-0.725	-0.369	-0.725	1.022
97	-0.725	-0.369	0.725	1.022
98	-0.725	0.369	-0.725	1.022
99	-0.725	0.369	0.725	1.022
100	-0.725	0.725	-0.369	1.022
101	-0.725	0.725	0.369	1.022
102	-0.369	-0.725	-0.725	1.022
103	-0.369	-0.725	0.725	1.022
104	-0.369	0.725	-0.725	1.022
105	-0.369	0.725	0.725	1.022
106	0.369	-0.725	-0.725	1.022
107	0.369	-0.725	0.725	1.022
108	0.369	0.725	-0.725	1.022
109	0.369	0.725	0.725	1.022
110	0.725	-0.725	-0.369	1.022
111	0.725	-0.725	0.369	1.022
112	0.725	-0.369	-0.725	1.022
113	0.725	-0.369	0.725	1.022
114	0.725	0.369	-0.725	1.022
115	0.725	0.369	0.725	1.022
116	0.725	0.725	-0.369	1.022
117	0.725	0.725	0.369	1.022
118	-0.725	-0.725	-0.725	1.462
119	-0.725	-0.725	0.725	1.462
120	-0.725	0.725	-0.725	1.462
121	-0.725	0.725	0.725	1.462

— continue on next page —

---

---

— continued from previous page —

#	x			y
122	0.725	-0.725	-0.725	1.462
123	0.725	-0.725	0.725	1.462
124	0.725	0.725	-0.725	1.462
125	0.725	0.725	0.725	1.462

---



**Table 8:** Local Minima of 1-Dimensional CosineMix

#	x	y
1	0.000	-0.100
2	-0.369	0.048
3	0.369	0.048
4	-0.725	0.487
5	0.725	0.487

**Table 9:** Local Minima of 2-Dimensional CosineMix

#	x	y
1	0.000	0.000
2	-0.369	0.000
3	0.000	-0.369
4	0.000	0.369
5	0.369	0.000
6	-0.369	-0.369
7	-0.369	0.369
8	0.369	-0.369
9	0.369	0.369
10	-0.725	0.000
11	0.000	-0.725
12	0.000	0.725
13	0.725	0.000
14	-0.725	-0.369
15	-0.725	0.369
16	-0.369	-0.725
17	-0.369	0.725
18	0.369	-0.725
19	0.369	0.725
20	0.725	-0.369
21	0.725	0.369
22	-0.725	-0.725
23	-0.725	0.725
24	0.725	-0.725
25	0.725	0.725

## A.4 HARTMANN Function

**Table 11:** Local Minima of 3-Dimensional HARTMANN

#	x			y
1	0.115	0.556	0.852	-3.863
2	0.109	0.860	0.564	-3.090
3	0.369	0.118	0.268	-1.001

**Table 12:** Local Minima of 6-Dimensional HARTMANN

#	x					y	
1	0.202	0.150	0.477	0.275	0.312	0.657	-3.322
2	0.405	0.882	0.846	0.574	0.139	0.038	-3.203

## A.5 HIMMELBLAU Function

**Table 13:** Local Minima of 2-Dimensional HIMMELBLAU

#	x		y
1	-3.779	-3.283	0.000
2	-2.805	3.131	0.000
3	3.000	2.000	0.000
4	3.584	-1.848	0.000

## A.6 Modified RASTRIGIN Function

**Table 14:** Local Minima of 4-Dimensional modified RASTRIGIN

#	x				y
1	0.249	0.249	0.166	0.125	0.789
2	0.249	0.249	0.166	0.374	1.786
3	0.249	0.249	0.498	0.125	2.118
4	0.249	0.746	0.166	0.125	2.779
5	0.746	0.249	0.166	0.125	2.779
6	0.249	0.249	0.498	0.374	3.115

— continue on next page —

---

— continued from previous page —

#	x				y
7	0.249	0.746	0.166	0.374	3.776
8	0.746	0.249	0.166	0.374	3.776
9	0.249	0.249	0.166	0.623	3.781
10	0.249	0.746	0.498	0.125	4.108
11	0.746	0.249	0.498	0.125	4.108
12	0.746	0.746	0.166	0.125	4.769
13	0.249	0.249	0.830	0.125	4.776
14	0.249	0.746	0.498	0.374	5.105
15	0.746	0.249	0.498	0.374	5.105
16	0.249	0.249	0.498	0.623	5.110
17	0.746	0.746	0.166	0.374	5.766
18	0.249	0.746	0.166	0.623	5.771
19	0.746	0.249	0.166	0.623	5.771
20	0.249	0.249	0.830	0.374	5.773
21	0.746	0.746	0.498	0.125	6.098
22	0.249	0.746	0.830	0.125	6.766
23	0.746	0.249	0.830	0.125	6.766
24	0.249	0.249	0.166	0.873	6.773
25	0.746	0.746	0.498	0.374	7.095
26	0.249	0.746	0.498	0.623	7.100
27	0.746	0.249	0.498	0.623	7.100
28	0.746	0.746	0.166	0.623	7.761
29	0.249	0.746	0.830	0.374	7.763
30	0.746	0.249	0.830	0.374	7.763
31	0.249	0.249	0.830	0.623	7.768
32	0.249	0.249	0.498	0.873	8.102
33	0.746	0.746	0.830	0.125	8.756
34	0.249	0.746	0.166	0.873	8.763
35	0.746	0.249	0.166	0.873	8.763
36	0.746	0.746	0.498	0.623	9.090
37	0.746	0.746	0.830	0.374	9.753
38	0.249	0.746	0.830	0.623	9.758
39	0.746	0.249	0.830	0.623	9.758
40	0.249	0.746	0.498	0.873	10.092
41	0.746	0.249	0.498	0.873	10.092
42	0.746	0.746	0.166	0.873	10.753
43	0.249	0.249	0.830	0.873	10.760
44	0.746	0.746	0.830	0.623	11.748

— continue on next page —

---

— continued from previous page —

#	x				y
45	0.746	0.746	0.498	0.873	12.082
46	0.249	0.746	0.830	0.873	12.750
47	0.746	0.249	0.830	0.873	12.750
48	0.746	0.746	0.830	0.873	14.740

**Table 15:** Local Minima of 8-Dimensional modified RASTRIGIN

#	x								y
1	0.495	0.249	0.495	0.249	0.495	0.166	0.495	0.125	2.769
2	0.495	0.249	0.495	0.249	0.495	0.166	0.495	0.374	3.766
3	0.495	0.249	0.495	0.249	0.495	0.498	0.495	0.125	4.098
4	0.495	0.249	0.495	0.746	0.495	0.166	0.495	0.125	4.759
5	0.495	0.746	0.495	0.249	0.495	0.166	0.495	0.125	4.759
6	0.495	0.249	0.495	0.249	0.495	0.498	0.495	0.374	5.095
7	0.495	0.249	0.495	0.746	0.495	0.166	0.495	0.374	5.756
8	0.495	0.746	0.495	0.249	0.495	0.166	0.495	0.374	5.756
9	0.495	0.249	0.495	0.249	0.495	0.166	0.495	0.623	5.761
10	0.495	0.249	0.495	0.746	0.495	0.498	0.495	0.125	6.088
11	0.495	0.746	0.495	0.249	0.495	0.498	0.495	0.125	6.088
12	0.495	0.746	0.495	0.746	0.495	0.166	0.495	0.125	6.748
13	0.495	0.249	0.495	0.249	0.495	0.830	0.495	0.125	6.756
14	0.495	0.249	0.495	0.746	0.495	0.498	0.495	0.374	7.085
15	0.495	0.746	0.495	0.249	0.495	0.498	0.495	0.374	7.085
16	0.495	0.249	0.495	0.249	0.495	0.498	0.495	0.623	7.090
17	0.495	0.746	0.495	0.746	0.495	0.166	0.495	0.374	7.746
18	0.495	0.249	0.495	0.746	0.495	0.166	0.495	0.623	7.751
19	0.495	0.746	0.495	0.249	0.495	0.166	0.495	0.623	7.751
20	0.495	0.249	0.495	0.249	0.495	0.830	0.495	0.374	7.753
21	0.495	0.746	0.495	0.746	0.495	0.498	0.495	0.125	8.077
22	0.495	0.249	0.495	0.746	0.495	0.830	0.495	0.125	8.746
23	0.495	0.746	0.495	0.249	0.495	0.830	0.495	0.125	8.746
24	0.495	0.249	0.495	0.249	0.495	0.166	0.495	0.873	8.753
25	0.495	0.746	0.495	0.746	0.495	0.498	0.495	0.374	9.075
26	0.495	0.249	0.495	0.746	0.495	0.498	0.495	0.623	9.080
27	0.495	0.746	0.495	0.249	0.495	0.498	0.495	0.623	9.080
28	0.495	0.746	0.495	0.746	0.495	0.166	0.495	0.623	9.741
29	0.495	0.249	0.495	0.746	0.495	0.830	0.495	0.374	9.743

— continue on next page —

— continued from previous page —

#	x							y	
30	0.495	0.746	0.495	0.249	0.495	0.830	0.495	0.374	9.743
31	0.495	0.249	0.495	0.249	0.495	0.830	0.495	0.623	9.748
32	0.495	0.249	0.495	0.249	0.495	0.498	0.495	0.873	10.082
33	0.495	0.746	0.495	0.746	0.495	0.830	0.495	0.125	10.735
34	0.495	0.249	0.495	0.746	0.495	0.166	0.495	0.873	10.743
35	0.495	0.746	0.495	0.249	0.495	0.166	0.495	0.873	10.743
36	0.495	0.746	0.495	0.746	0.495	0.498	0.495	0.623	11.070
37	0.495	0.746	0.495	0.746	0.495	0.830	0.495	0.374	11.733
38	0.495	0.249	0.495	0.746	0.495	0.830	0.495	0.623	11.738
39	0.495	0.746	0.495	0.249	0.495	0.830	0.495	0.623	11.738
40	0.495	0.249	0.495	0.746	0.495	0.498	0.495	0.873	12.072
41	0.495	0.746	0.495	0.249	0.495	0.498	0.495	0.873	12.072
42	0.495	0.746	0.495	0.746	0.495	0.166	0.495	0.873	12.733
43	0.495	0.249	0.495	0.249	0.495	0.830	0.495	0.873	12.740
44	0.495	0.746	0.495	0.746	0.495	0.830	0.495	0.623	13.728
45	0.495	0.746	0.495	0.746	0.495	0.498	0.495	0.873	14.062
46	0.495	0.249	0.495	0.746	0.495	0.830	0.495	0.873	14.730
47	0.495	0.746	0.495	0.249	0.495	0.830	0.495	0.873	14.730
48	0.495	0.746	0.495	0.746	0.495	0.830	0.495	0.873	16.720

## A.7 SHEKEL Function

**Table 16:** Local Minima of 5-Parametric SHEKEL

#	x				y
1	4.000	4.000	4.000	4.000	-10.153
2	8.000	8.000	8.000	8.000	-5.101
3	1.000	1.000	1.000	1.000	-5.055
4	5.999	6.000	5.999	6.000	-2.683
5	3.002	6.998	3.002	6.998	-2.630

**Table 17:** Local Minima of 7-Parametric SHEKEL

#	x				y
1	4.000	4.000	4.000	4.000	-10.403
2	8.000	8.000	8.000	8.000	-5.129
3	1.000	1.000	1.000	1.000	-5.088
4	4.995	3.006	4.995	3.006	-3.703
5	5.998	5.999	5.998	5.999	-2.752
6	3.001	7.001	3.001	7.001	-2.750
7	2.005	8.992	2.005	8.992	-1.833



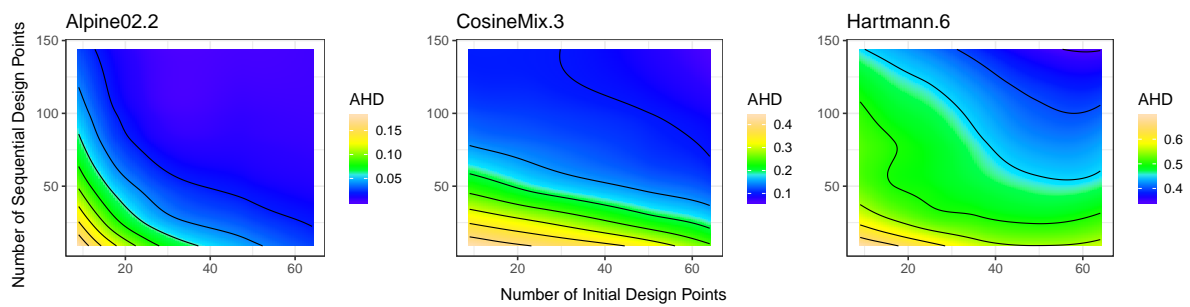
**Table 18:** Local Minima of 10-Parametric SHEKEL

#	x				y
1	4.000	4.000	4.000	4.000	-10.536
2	8.000	8.000	8.000	8.000	-5.176
3	1.000	1.000	1.000	1.000	-5.128
4	5.002	3.002	5.002	3.002	-4.070
5	5.999	5.997	5.999	5.997	-2.871
6	3.001	7.000	3.001	7.000	-2.790
7	5.992	2.022	5.992	2.022	-2.608
8	6.986	3.593	6.986	3.593	-2.495
9	2.005	8.991	2.005	8.991	-1.854
10	7.985	1.013	7.985	1.013	-1.696

## B Contour Plots

Contour plots of the performance measurements peak ratio (PR) and averaged HAUSDORFF distance (AHD) over the number of initial and sequential design points for infill criteria GEILM are shown in this section. Each contour line is smoothed by LOESS (CLEVELAND; GROSSE and SHYU 2017).

### B.1 Showcases

**Figure 5:** Contour Plot of AHD

## B.2 All Objective Functions

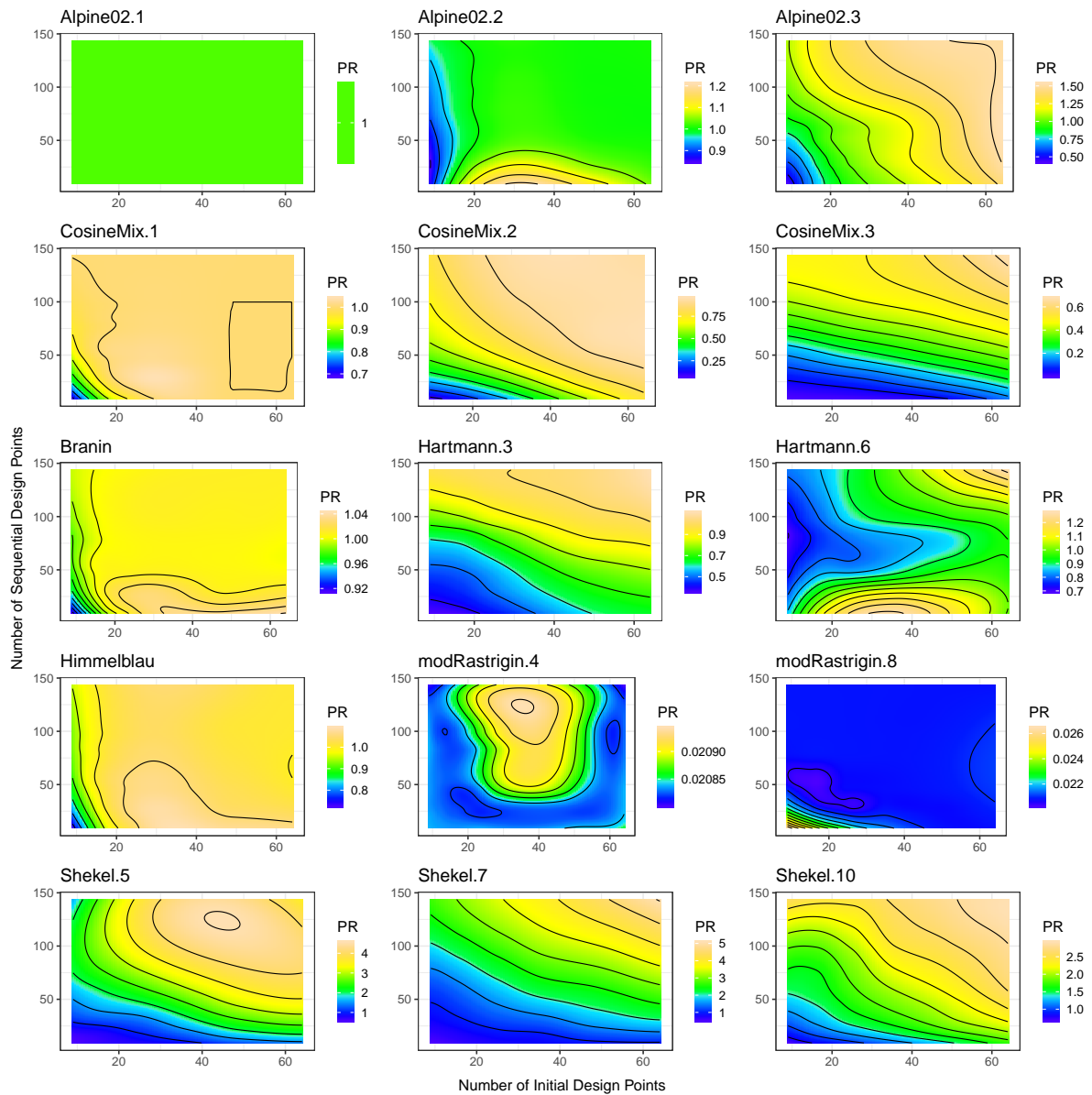


Figure 6: Contour Plot of PR for all Objective Functions

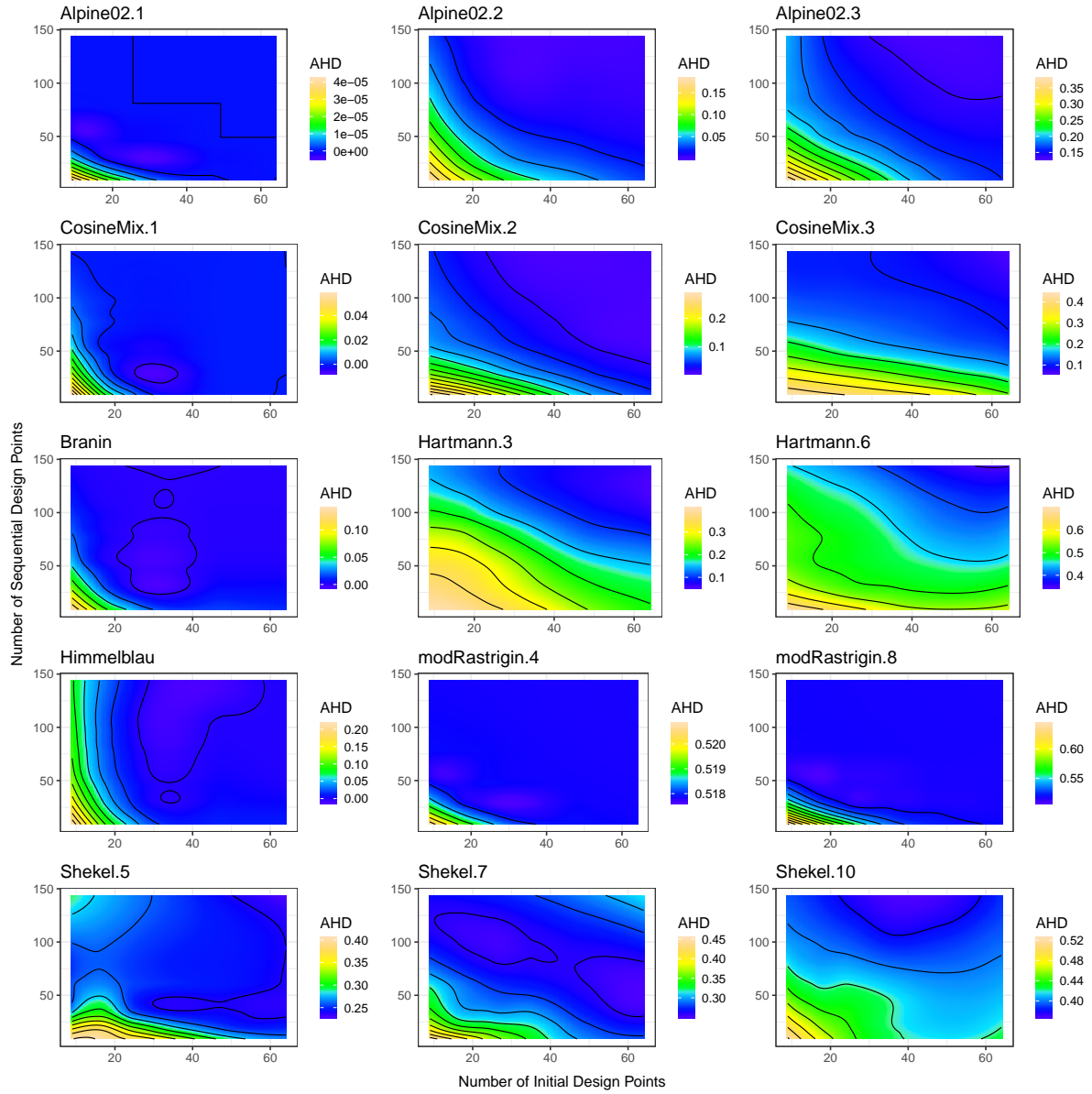


Figure 7: Contour Plot of AHD for all Objective Functions

## References

- ABBAS, Syed Ali; Raza SAMAR; M. A. RIZVI and Aamer Iqbal BHATTI (2018): 'A Method for Multimodal Optimization with Application to Signal Processing'. In: IEEE, pp. 357–364. ISBN: 978-1-5386-3564-3. DOI: [10.1109/IBCAST.2018.8312249](https://doi.org/10.1109/IBCAST.2018.8312249) (cit. on p. 6).
- ABELLO, James M.; P. M. PARDALOS and Mauricio G. C. RESENDE, eds. (2002): *Handbook of Massive Data Sets*. Massive Computing 4. Dordrecht; London: Kluwer Academic. ISBN: 978-1-4020-0489-6 (cit. on p. 6).
- ALI, M. Montaz; Charoenchai KHOMPATRAPORN and Zelda B. ZABINSKY (2005): 'A Numerical Evaluation of Several Stochastic Algorithms on Selected Continuous Global Optimization Test Problems'. In: *Journal of Global Optimization* 31.4, pp. 635–672. ISSN: 0925-5001, 1573-2916. DOI: [10.1007/s10898-004-9972-2](https://doi.org/10.1007/s10898-004-9972-2) (cit. on p. 7).
- BISCHL, Bernd; Jakob RICHTER; Jakob BOSSEK; Daniel HORN; Janek THOMAS and Michel LANG (2017): 'mlrMBO: A Modular Framework for Model-Based Optimization of Expensive Black-Box Functions'. In: arXiv: [1703.03373 \[stat\]](https://arxiv.org/abs/1703.03373). URL: <http://arxiv.org/abs/1703.03373v2> (cit. on pp. 2, 3, 8).
- BISCHL, Bernd; Simon WESSING; Nadja BAUER; Klaus FRIEDRICHS and Claus WEIHS (2014): 'MOI-MBO: Multiobjective Infill for Parallel Model-Based Optimization'. In: *Learning and Intelligent Optimization*. Vol. 8426. Cham: Springer International Publishing, pp. 173–186. ISBN: 978-3-319-09583-7. DOI: [10.1007/978-3-319-09584-4\\_17](https://doi.org/10.1007/978-3-319-09584-4_17) (cit. on p. 2).
- BYRD, Richard H.; Peihuang LU; Jorge NOCEDAL and Ciyou ZHU (1995): 'A Limited Memory Algorithm for Bound Constrained Optimization'. In: *SIAM Journal on Scientific Computing* 16.5, pp. 1190–1208. DOI: [10.1137/0916069](https://doi.org/10.1137/0916069) (cit. on p. 5).
- CLERC, Maurice (1999): 'The Swarm and the Queen: Towards a Deterministic and Adaptive Particle Swarm Optimization'. In: IEEE, pp. 1951–1957. ISBN: 978-0-7803-5536-1. DOI: [10.1109/CEC.1999.785513](https://doi.org/10.1109/CEC.1999.785513) (cit. on p. 7).
- CLEVELAND, William S.; Eric GROSSE and William M. SHYU (2017): 'Local Regression Models'. In: *Statistical Models in S*. Ed. by HASTIE, T. J. OCLC: 1011109593. New York, p. 68. ISBN: 978-1-351-41423-4 (cit. on pp. 9, 27).
- DEB, Kalyanmoy and Amit SAHA (2010): 'Finding Multiple Solutions for Multimodal Optimization Problems Using a Multi-Objective Evolutionary Approach'. In: *Genetic and Evolutionary Computation*. ACM Press, pp. 447–454. ISBN: 978-1-4503-0072-8. DOI: [10.1145/1830483.1830568](https://doi.org/10.1145/1830483.1830568) (cit. on p. 6).
- DEB, Kalyanmoy and Amit SAHA (2012): 'Multimodal Optimization Using a Bi-Objective Evolutionary Algorithm'. In: *Evolutionary Computation* 20.1, pp. 27–62. ISSN: 1063-6560. DOI: [10.1162/EVC0\\_a\\_00042](https://doi.org/10.1162/EVC0_a_00042) (cit. on p. 7).
- DIXON, L. C. W. and G. P. SZEGÖ, eds. (1978): *Towards Global Optimisation* 2. Amsterdam: North-Holland. ISBN: 978-0-444-85171-0 (cit. on p. 7).

- GUDLA, Pradeep Kumar and Ranjan GANGULI (2005): 'An Automated Hybrid Genetic-Conjugate Gradient Algorithm for Multimodal Optimization Problems'. In: *Applied Mathematics and Computation* 167.2, pp. 1457–1474. ISSN: 00963003. DOI: [10.1016/j.amc.2004.08.026](https://doi.org/10.1016/j.amc.2004.08.026) (cit. on p. 6).
- HAUSDORFF, Felix (1927): *Mengenlehre*. Berlin (cit. on p. 6).
- HIMMELBLAU, David Mautner (1972): *Applied Nonlinear Programming*. McGraw-Hill Companies (cit. on p. 7).
- JONES, Donald R.; Matthias SCHONLAU and William J. WELCH (1998): 'Efficient Global Optimization of Expensive Black-Box Functions'. In: *Journal of Global Optimization* 13.4, pp. 455–492. ISSN: 1573-2916. DOI: [10.1023/A:1008306431147](https://doi.org/10.1023/A:1008306431147) (cit. on pp. 2, 3).
- LANG, Michel; Bernd BISCHL and Dirk SURMANN (2017): 'Batchtools: Tools for R to Work on Batch Systems'. In: *The Journal of Open Source Software* 2.10, p. 135. ISSN: 2475-9066. DOI: [10.21105/joss.00135](https://doi.org/10.21105/joss.00135). URL: <http://joss.theoj.org/papers/10.21105/joss.00135> (visited on 07/11/2018) (cit. on p. 8).
- MCKAY, M. D.; R. J. BECKMAN and W. J. CONOVER (1979): 'A Comparison of Three Methods for Selecting Values of Input Variables in the Analysis of Output from a Computer Code'. In: *Technometrics* 21.2, pp. 239–245. ISSN: 00401706. DOI: [10.2307/1268522](https://doi.org/10.2307/1268522) (cit. on p. 3).
- NOCEDAL, Jorge and Stephen J. WRIGHT (2006): *Numerical Optimization*. 2nd ed. Springer Series in Operations Research. New York: Springer. ISBN: 978-0-387-98793-4 (cit. on p. 5).
- R DEVELOPMENT CORE TEAM (2017): *R: A Language and Environment for Statistical Computing*. Version 3.4.3. URL: <http://www.r-project.org/> (cit. on p. 8).
- ROCKAFELLAR, R. Tyrrell and Roger J.-B. WETS (2004): *Variational Analysis*. Corr. 2nd print. Grundlehren der mathematischen Wissenschaften 317. Berlin: Springer. ISBN: 978-3-540-62772-2 (cit. on p. 6).
- STEIN, Michael (1987): 'Large Sample Properties of Simulations Using Latin Hypercube Sampling'. In: *Technometrics* 29.2, pp. 143–151. ISSN: 00401706. DOI: [10.2307/1269769](https://doi.org/10.2307/1269769) (cit. on pp. 5, 7).
- STOEAN, Catalin; Mike PREUSS; Ruxandra STOEAN and D. DUMITRESCU (2010): 'Multimodal Optimization by Means of a Topological Species Conservation Algorithm'. In: *IEEE Transactions on Evolutionary Computation* 14.6, pp. 842–864. ISSN: 1089-778X, 1941-0026. DOI: [10.1109/TEVC.2010.2041668](https://doi.org/10.1109/TEVC.2010.2041668) (cit. on p. 6).
- SURMANN, Dirk; Uwe LIGGES and Claus WEIHS (2014): 'Modelling Low Frequency Oscillations in an Electrical System'. In: *Energy Conference (ENERGYCON), 2014 IEEE International*. Dubrovnik, Croatia: IEEE, pp. 565–571. DOI: [10.1109/ENERGYCON.2014.6850482](https://doi.org/10.1109/ENERGYCON.2014.6850482) (cit. on p. 1).

- SURMANN, Dirk; Uwe LIGGES and Claus WEIHS (2017): 'Predicting Measurements at Unobserved Locations in an Electrical Transmission System'. In: *Computational Statistics*. ISSN: 1613-9658. DOI: [10.1007/s00180-017-0734-2](https://doi.org/10.1007/s00180-017-0734-2) (cit. on p. 1).
- TÖRN, Aimo and Sami VIITANEN (1992): 'Topographical Global Optimization'. In: *Recent Advances in Global Optimization*. Ed. by FLOUDAS, Christodoulos A. and PARDALOS, Panos M. Princeton Series in Computer Sciences. Princeton University Press, pp. 384–398 (cit. on pp. 2, 5).
- URSEM, R. K. (1999): 'Multinational Evolutionary Algorithms'. In: IEEE, pp. 1633–1640. ISBN: 978-0-7803-5536-1. DOI: [10.1109/CEC.1999.785470](https://doi.org/10.1109/CEC.1999.785470) (cit. on p. 6).
- WESSING, Simon and Mike PREUSS (2017): 'The True Destination of EGO Is Multi-Local Optimization'. In: arXiv: [1704.05724](https://arxiv.org/abs/1704.05724) [math, cs]. URL: <http://arxiv.org/abs/1704.05724v1> (cit. on pp. 2, 3, 5).
- WILLIAMS, Christopher K.I. and Carl Edward RASMUSSEN (2006): 'Gaussian Processes for Machine Learning'. In: *MIT Press* (cit. on p. 3).